Supplemental Data

Structure, Dynamics, and Ionization Equilibria of the Tyrosine Residues in *Bacillus circulans* Xylanase

Simon J. Baturin, Mark Okon, and Lawrence P. McIntosh*

Department of Biochemistry and Molecular Biology, Department of Chemistry, and Michael Smith Laboratories, University of British Columbia, Vancouver BC, V6T 1Z3, Canada

*Corresponding author:
Lawrence P. McIntosh
Department of Biochemistry and Molecular Biology
Life Sciences Centre, 2350 Health Sciences Mall
University of British Columbia
Vancouver, B.C.
Canada, V6T 1Z3
Phone: (001) 604-822-3341
Fax: (001) 604-822-5227
E-mail: mcintosh@chem.ubc.ca

Table S1. BcX tyrosine chemical shifts (ppm) [a]

Tyrosine	$^{13}C^{\beta}$	$^{1}H^{\delta}$ / $^{13}C^{\delta}$	$^{1}H^{\varepsilon}$ / $^{13}C^{\varepsilon}$	$^{13}C^{\zeta}$	$^{1}H^{\eta}$
Y5	42.20	6.72 / 132.94	6.23 / 118.12	156.92	
Y26	43.00	6.99 / 134.00	6.74 / 119.01	158.89	7.80
Y53	41.25	6.64 / 132.77	6.55 / 118.07	158.76	11.50
Y65	42.73	7.32 / 131.26	6.96 / 119.31	158.08	
Y69	43.40	6.09 / 131.80	6.57 / 118.00	158.06	
Y79 [b]	42.41	6.18 / 133.60 6.70 / 132.61	6.00 / 115.83 5.79 / 118.66	156.80	9.64
Y80 [c]	-	-	-	-	
Y88	40.99	7.12 / 133.35	6.62 / 118.22	157.33	
Y94	39.26	6.85 / 132.56	6.76 / 119.01	157.35	
Y105 [b]	39.70	7.32 / 133.0 6.94 / 133.02	7.63 / 120.10 7.27 / 119.24	158.45	12.53
Y108	43.80	6.58 / 133.53	6.69 / 118.41	158.01	
Y113	40.95	7.05 / 133.85	6.70 / 117.83	157.20	
Y128 [c]	-	-	-	-	
Y166	38.51	6.73 / 132.97	6.53 / 117.88	158.71	
Y174	40.27	6.84 / 132.27	6.75 / 118.45	157.49	

[a] BcX in 10 mM sodium phosphate, pH 6.5, at 25 °C. Chemical shifts referenced directly to external DSS.

[b] Top (bottom) rows are for δ1/ε1 (and δ2/ε2).

[c] Could not be assigned reliably.

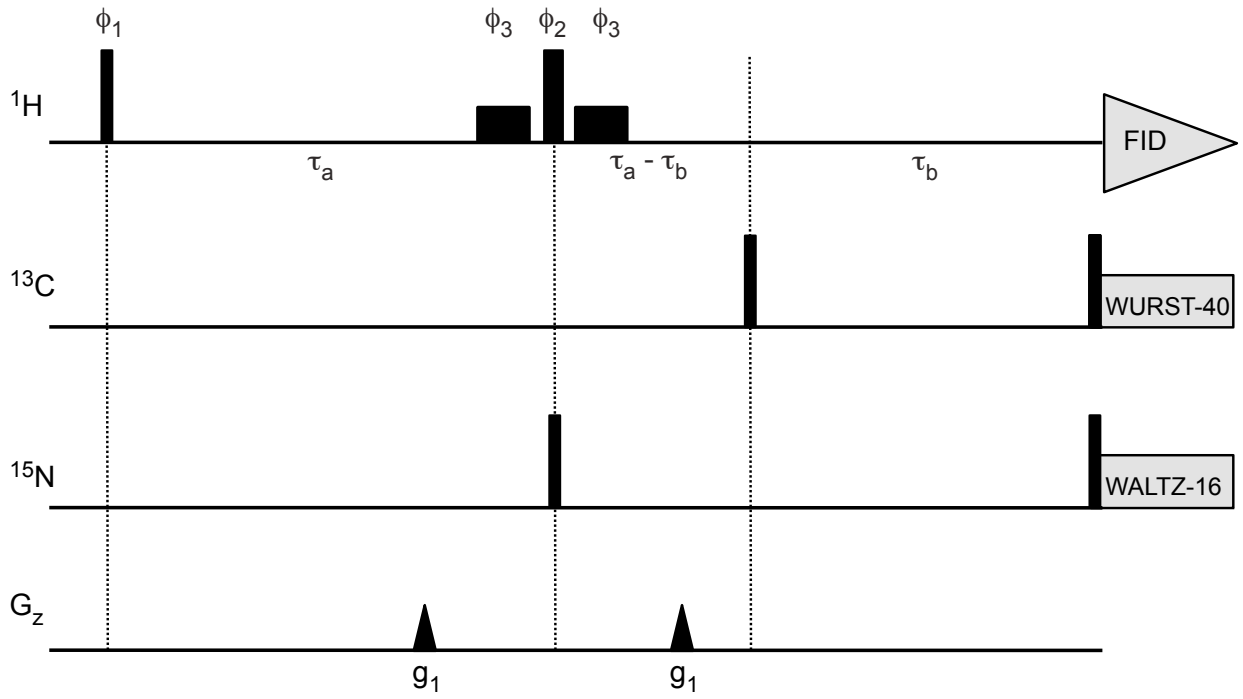

Fig. S1. Pulse sequence for a 1D $^{13}C/^{15}N$-filtered experiment to detect signals from ^{1}H nuclei bonded directly to oxygen (or sulfur) atoms while suppressing those bonded directly to amide ^{15}N or aromatic ^{13}C nuclei (see Figures 1 and 4). Frequencies: ^{1}H, 4.8 ppm (water); ^{13}C, 126 ppm (aromatic region); ^{15}N, 118 ppm (amide region). Delays: τ_a = 5.3 ms and τ_b = 3.1 ms. Hard 90° (180°) pulses are depicted by tall narrow (wide) rectangles, and the 1.8 ms selective ^{1}H 180° WATERGATE pulses as short rectangles. The triangles indicate 200 μs trapezoidal shape gradients at 46.9 G/cm (g_1). Although not required, ^{13}C (2.36 kHz, WURST-40) and ^{15}N (0.94 kHz, WALTZ-16) decoupling during acquisition improves filtering.

The phase cycling is:
ϕ_1 = 4(x, -x), 4(y, -y), 4(-x, x), 4(-y, y)
ϕ_2 = 2(x), 2(y), 2(-x), 2(-y), 2(y), 2(-x), 2(-y), 2(x), 2(-x), 2(-y), 2(x), 2(y), 2(-y), 2(x), 2(y), 2(-x)
ϕ_3 = 2(-x), 2(-y), 2(x), 2(y), 2(-y), 2(x), 2(y), 2(-x), 2(x), 2(y), 2(-x), 2(-y), 2(y), 2(-x), 2(-y), 2(x)
receiver = 2(x, -x, -x, x), 2(y, -y, -y, y), 2(-x, x, x, -x), 2(-y, y, y, -y)

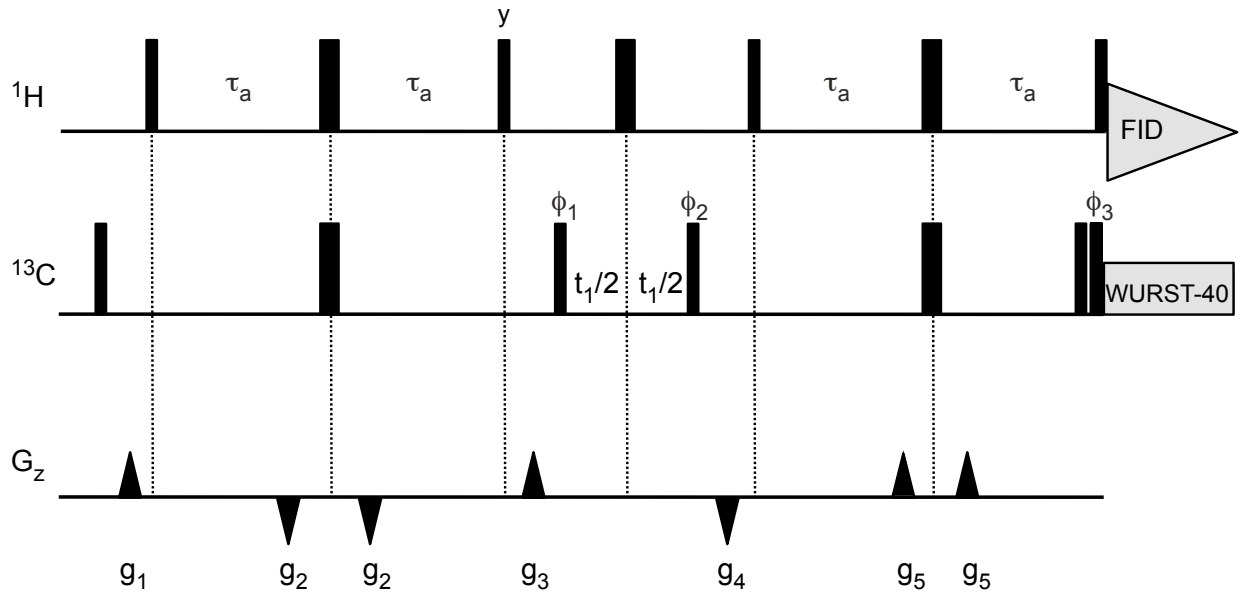

Fig. S2. Pulse sequence for a long-range 2D ^{13}C-HSQC experiment to detect tyrosine $^1H^{\eta}$ - $^{13}C^{\varepsilon}$ (and weaker $^1H^{\eta}$-$^{13}C^{\zeta}$) correlations and suppress direct ^{1}H-^{13}C correlations (see Figures 1, 2 and 7). Frequencies: ^{1}H, 4.8 ppm (water); ^{13}C, 126 ppm (aromatic region). Spectral widths: ^{1}H, 15000 Hz; ^{13}C, 9654 Hz (96 complex t_1 increments) with a 600 MHz spectrometer. Delay τ_a = 9.4 ms (or integer multiples of 1/(2*160 Hz)). Hard 90° (180°) pulses are depicted by narrow (wide) rectangles. The triangles indicate trapezoidal shape z-gradients: g_1 = 500 μs, 1.8 G/cm; g_2 = 300 μs, -18.8 G/cm; g_3 = 1.5 ms, 28.0 G/cm; g_4 = 600 μs, -35.6 G/cm; and g_5 = 200 μs, 26.2 G/cm. Decoupling during acquisition (84 ms) is achieved with a 2.36 kHz WURST-40 field.

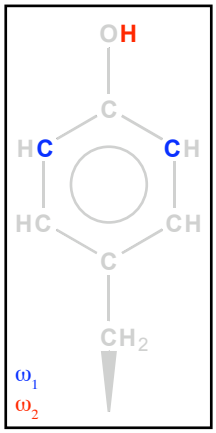

Pulses are applied along the x-axis except where indicated. The phase cycling is:
ϕ_1 = x, -x (plus States-TPPI incrementation for quadrature detection in t_1)
ϕ_2 = 2(x), 2(-x)
ϕ_3 = 4(x), 4(-x)
receiver = x, -x, -x, x

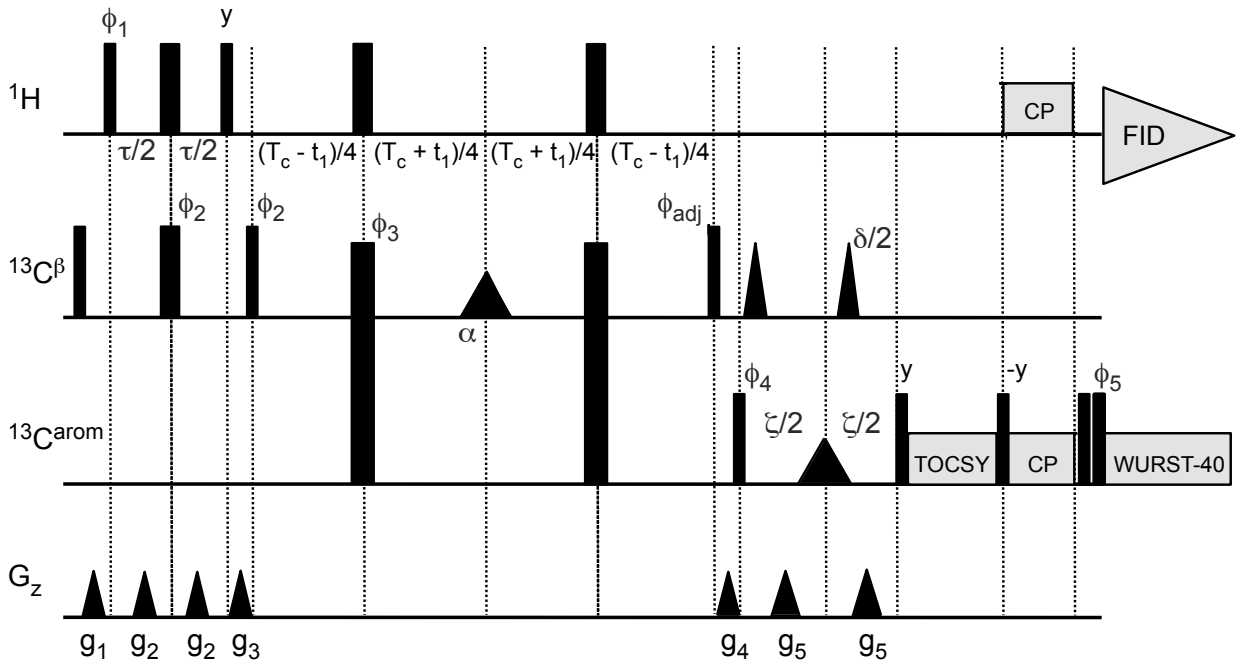

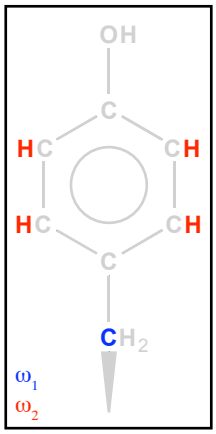

Fig. S3. Pulse sequence for a 2D $C^{\beta}(C^{\gamma}CC\text{-}TOCSY)H^{ar}$ experiment to detect $^{13}C^{\beta}$-aromatic ring ^{1}H correlations (adapted from (Löhr et al. 2005) and (Löhr et al. 2007)). Frequencies: ^{1}H, 4.8 ppm (water); ^{13}C, initially 35.5 ppm ($^{13}C^{\beta}$) then switched to 132.2 ppm (aromatic region). Spectral widths: ^{1}H, 6993 Hz; ^{13}C, 4223 Hz (35 complex t_1 increments) with a 600 MHz spectrometer. Delays: constant time T_c = 8.5 ms, τ = 3.4 ms, δ = 10.4 ms, and ζ = 14 ms. Hard 90° (180°) pulses are depicted by narrow (wide) rectangles, and selective pulses as triangles or long filled bars. The tall filled bars are 500 μs 180° broadband WURST-10 pulses. The pulse labelled α is a 2.5 ms selective 180° I-BURP-2 at 58 ppm ($^{13}C^{\alpha}$ region). The 2.7 ms 180° RE-BURP pulse in the middle of the ζ period is applied at 129 ppm. The two 180° phase modulated pulses on $^{13}C^{\beta}$ in the ζ period have the shape of the centre lobe of a sinc-function and a duration of 150 μs. The ^{13}C-TOCSY consists of one cycle of a 3.3 kHz DIPSI-2. The ^{13}C-^{1}H polarization transfer (CP) consists of one cycle of a 5.4 kHz DIPSI-2. The trapezoidal shape z-gradients have a duration of 500 μs and strengths: g_1 = 7.5 G/cm; g_2 = 5.6 G/cm; g_3 = 14.0 G/cm; g_4 = 9.4 G/cm; and g_5 = 6.1 G/cm. Decoupling during acquisition (88 ms) is achieved with a 2.36 kHz WURST-40 field.

Pulses are applied along x-axis except where indicated. The phase cycling is:
ϕ_1 = 4(x), 4(-x)
ϕ_2 = 2(x), 2(-x) (plus States-TPPI incrementation for quadrature detection in t_1)
ϕ_3 = x, y
ϕ_4 = 8(x), 8(-x)
ϕ_5 = 16(x), 16(-x)
ϕ_{adj} was adjusted to 84° for optimal signal
receiver = (x, -x, -x, x), 2(-x,x,x,-x), (x, -x, -x, x)

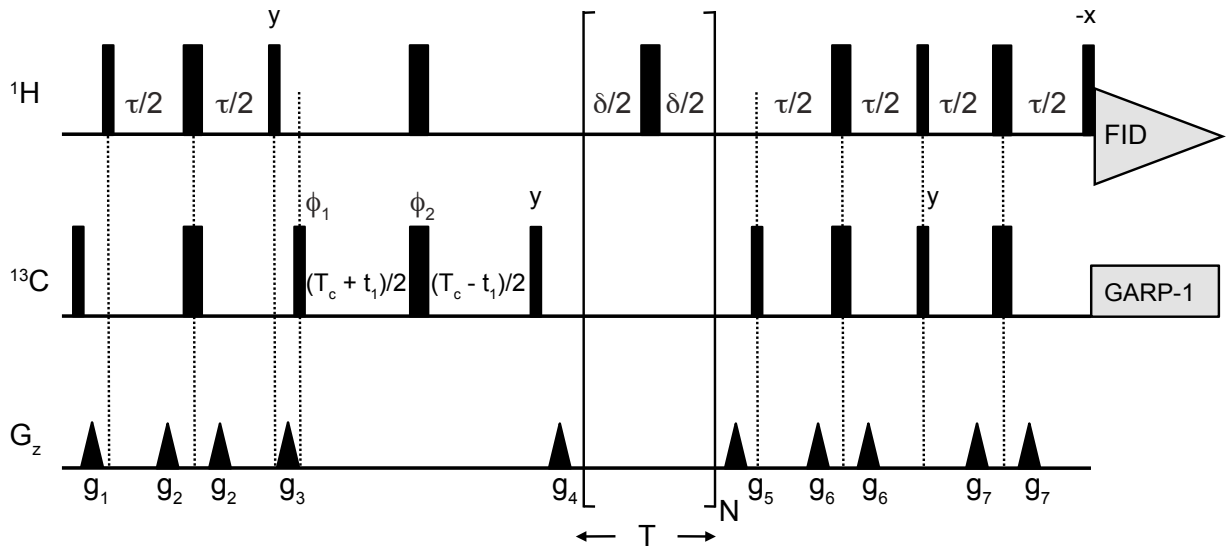

Fig. S4. Pulse sequence for the simultaneous measurement of tyrosine longitudinal ^{13}C decay and conformational exchange rates (constant time version, adapted from (Farrow et al. 1994); see Figure 5). Frequencies: ^{1}H, 4.8 ppm (water); ^{13}C, 125 ppm (aromatic region). Spectral widths: ^{1}H, 10000 Hz; ^{13}C, 4080 Hz (64 complex t_1 increments) with a 600 MHz spectrometer. Delays: constant time T_c = 15.8 ms, τ = 2.5 ms, and δ = 5 ms. Mixing period delays T are multiples of N to give 10, 50, 100, 200, 300, 400, 600, 800 and 1000 ms. Hard 90^o (180^o) pulses are depicted by narrow (wide) rectangles. The triangles indicate trapezoidal shape z-gradients: g_1 = 1 ms, 9.4 G/cm; g_2 = 0.5 ms, 7.5 G/cm; g_3 = 1 ms, 28.1 G/cm; g_4 = 1 ms, -37.5 G/cm; g_5 = 0.5 ms, -43.1 G/cm; g_6 = 0.5 ms, 15.0 G/cm; g_7 = 0.2 ms, -46.8 G/cm. Decoupling during acquisition (64 ms) is achieved with a 1.74 kHz GARP-1 field.

Pulses are applied along x-axis except where indicated. The phase cycling is:
ϕ_1 = x (plus States-TPPI incrementation for quadrature detection in t_1)
ϕ_2 = x, y, -x, -y
receiver = x, -x

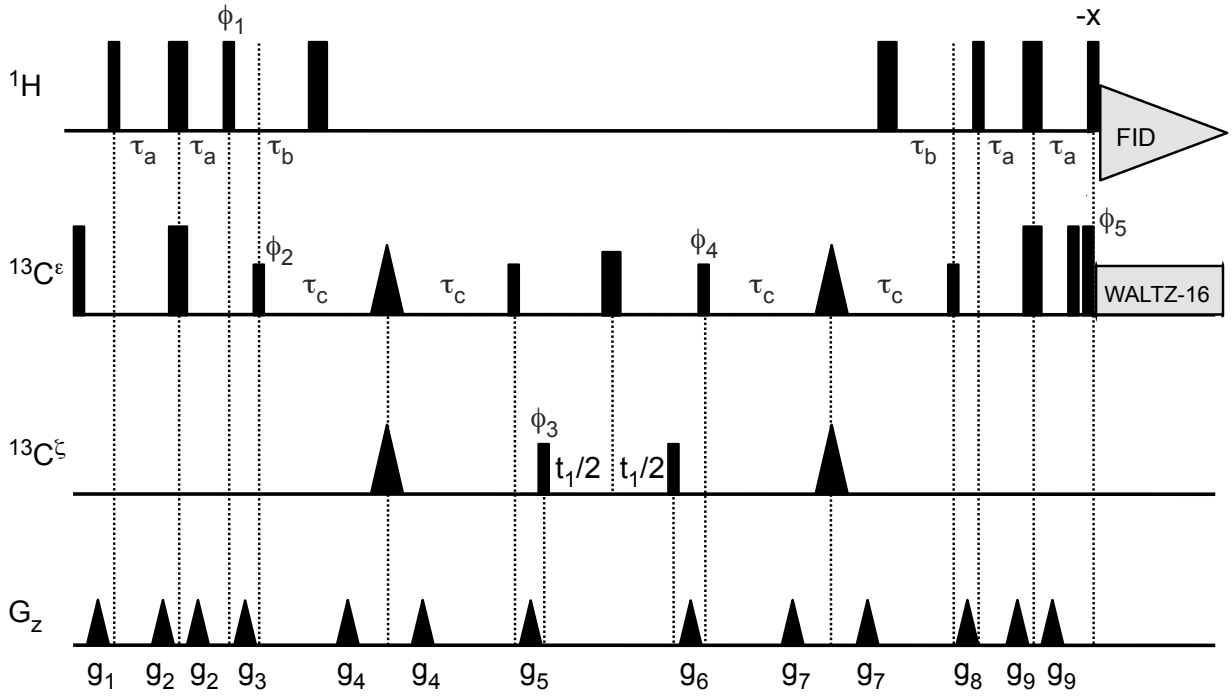

Fig. S5. The pulse sequence for a two-dimensional $^{13}C^{\zeta}(^{13}C^{\varepsilon})^{1}H^{\varepsilon}$ experiment to correlate tyrosine $^{1}H^{\varepsilon}$ and $^{13}C^{\zeta}$ signals (see Figure 6C). The magnetization transfer follows an "out-and-back" pathway: $^{1}H^{\varepsilon} \rightarrow {}^{13}C^{\varepsilon} \rightarrow {}^{13}C^{\zeta}(t_1) \rightarrow {}^{13}C^{\varepsilon} \rightarrow {}^{1}H^{\varepsilon}(t_2)$. Frequencies: ^{1}H, 4.8 ppm (water); ^{13}C, 118 ppm ($^{13}C^{\varepsilon}$) and switched to 157.7 ppm ($^{13}C^{\zeta}$) during the t_1 period. Spectral widths: ^{1}H, 8403 Hz; ^{13}C, 754 Hz (40 complex t_1 increments) with a 600 MHz spectrometer. Delays: τ_a = 1.4 ms, τ_b = 1.35 ms, and τ_c = 3.45 ms (and the last delay includes half the duration of the 180° selective 2.9 ms RE-BURP pulse). Hard 90° (180°) pulses are depicted by narrow (wide) rectangles, and shaped pulses are triangles. The first two and last three carbon hard pulses are applied with full power (B_1 = 15.8 kHz), whereas the remaining carbon hard 90° pulses are selective (B_1 = 1.546 kHz). The first and last carbon shaped 180° pulses are selective 2.9 ms RE-BURP with maximum excitations at 118 ppm ($^{13}C^{\varepsilon}$) and 157.7 ppm ($^{13}C^{\zeta}$). The 180° 144 μs rectangular pulse in the middle of the t_1 period has a maximum excitation at 118 ppm ($^{13}C^{\varepsilon}$). Shaped pulses were constructed with the Varian Pbox utility. The triangles indicate trapezoidal shaped z-gradients: g_1 = 500 μs, 8.1 G/cm; g_2 = 500 μs, 6.1 G/cm; g_3 = 3 ms, 15.2 G/cm; g_4 = 200 μs, 7.6 G/cm; g_5 = 750 μs, 5.6 G/cm; g_6 = 500 μs, 10.1 G/cm; g_7 = 200 μs, 6.6 G/cm; g_8 = 500 μs, 16.2 G/cm; g_9 = 500 μs, 60.8 G/cm. Decoupling during acquisition (86 ms) is achieved with a 2.36 kHz WALTZ-16 field.

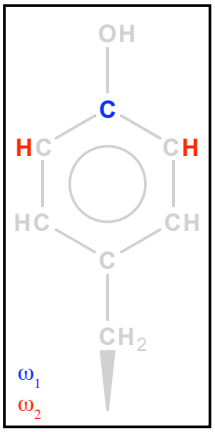

Pulses are applied along x-axis except where indicated. The phase cycling is:
ϕ_1 = 8(x), 8(-x)
ϕ_2 = 2(x), 2(-x)
ϕ_3 = x, -x (plus States-TPPI incrementation for quadrature detection in t_1)
ϕ_4 = 4(x), 4(-x)
ϕ_5 = 16(x), 16(-x)
receiver = x, 2(-x), x, -x, 2(x), 2(-x), 2(x), -x, x, 2(-x), x.

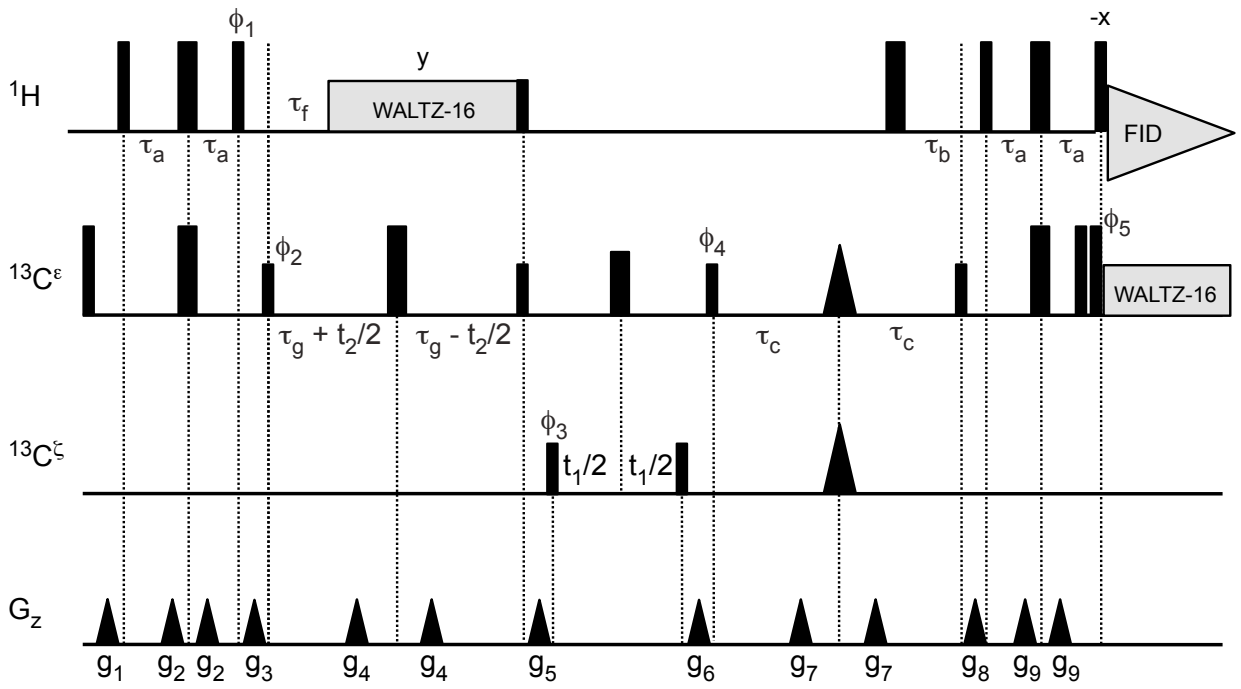

Fig. S6. The pulse sequence for a three-dimensional $^{13}C^{\zeta}{}^{13}C^{\varepsilon}{}^{1}H^{\varepsilon}$ experiment to correlate tyrosine $^{1}H^{\varepsilon}$, $^{13}C^{\varepsilon}$ and $^{13}C^{\zeta}$ signals (see Figure 6D). The magnetization transfer pathway is $^{1}H^{\varepsilon} \rightarrow {}^{13}C^{\varepsilon}(t_2) \rightarrow {}^{13}C^{\zeta}(t_1) \rightarrow {}^{13}C^{\varepsilon} \rightarrow {}^{1}H^{\varepsilon}(t_3)$. Due to the non-selective character of the 180° ^{13}C pulse applied inside the $2*\tau_g$ delay for constant time t_2 evolution, only half of the magnetization originating from $^{1}H^{\varepsilon}$ is returned. All parameters are the same as for the two-dimensional $^{13}C^{\zeta}(^{13}C^{\varepsilon})^{1}H^{\varepsilon}$ (Figure S5) with the following exceptions: additional delays $\tau_f = 2*\tau_b$ and $\tau_g = 19$ ms; $^{13}C^{\varepsilon}$ spectral width 903 Hz, 25 complex t_1 increments, and 17 complex t_2 increments; ^{1}H decoupling (8.3 kHz) and ^{13}C decoupling (2.2 kHz) are accomplished with WALTZ-16 modulation.

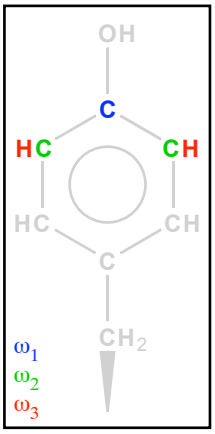

Quadrature detection in t_1 and t_2 is obtained by States-TPPI incrementation of ϕ_3 and ϕ_2, respectively.

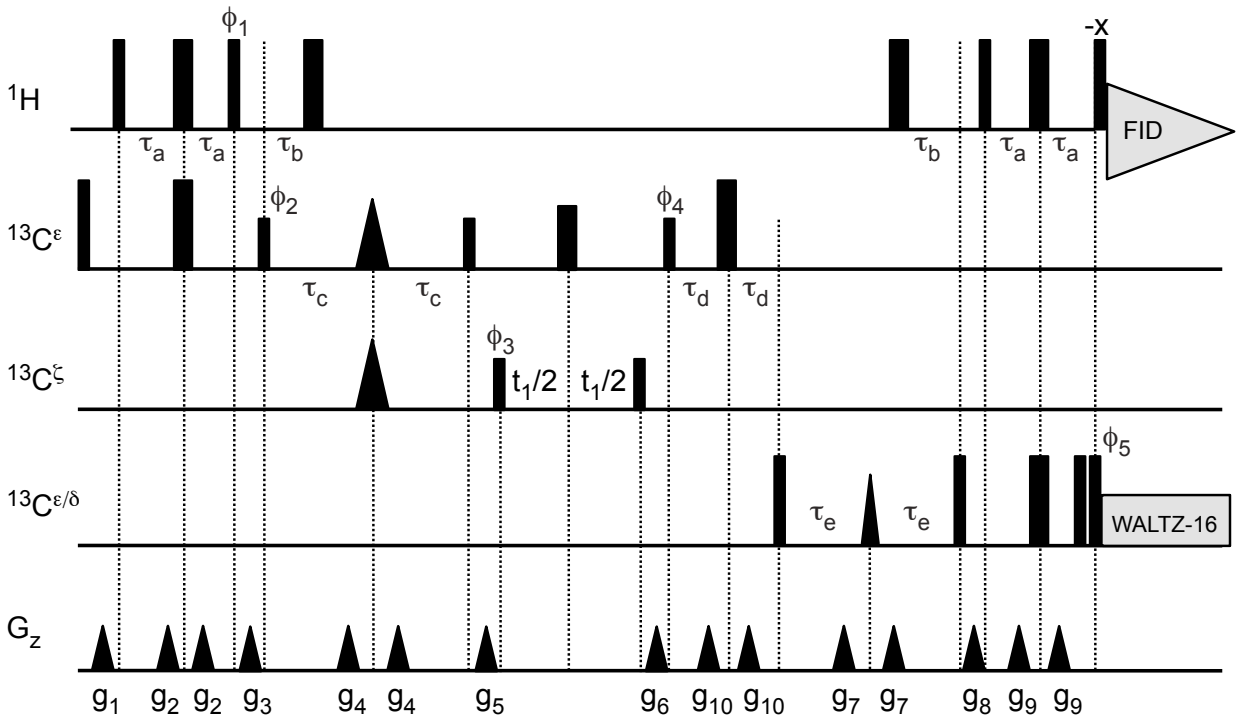

Fig. S7. The pulse sequence for a two-dimensional $^{13}C^{\zeta}(^{13}C^{\varepsilon/\delta})^{1}H^{\varepsilon/\delta}$ experiment to correlate tyrosine $^{1}H^{\varepsilon/\delta}$ and $^{13}C^{\zeta}$ signals (see Figure 6A). The magnetization transfer pathway is:

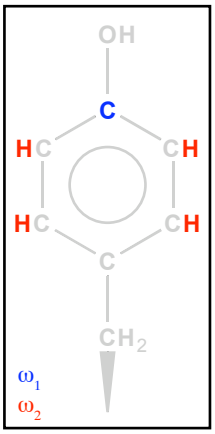

$$^{1}H^{\varepsilon}\ (t_2)$$
$$\uparrow$$
$$^{1}H^{\varepsilon} \rightarrow {}^{13}C^{\varepsilon} \rightarrow {}^{13}C^{\zeta}\ (t_1) \rightarrow {}^{13}C^{\varepsilon} \rightarrow {}^{13}C^{\delta} \rightarrow {}^{1}H^{\delta}\ (t_2)$$

All parameters are the same as for the two-dimensional $^{13}C^{\zeta}(^{13}C^{\varepsilon})^{1}H^{\varepsilon}$ (Figure S5) with the following exceptions: delays $2*\tau_d = 5.6$ msec and $2*\tau_e = 4$ ms (the last delay includes the duration of the 180° ^{13}C selective 490 μs R-SNOB pulse); $^{1}H^{\varepsilon/\delta}$ spectral width: 8403.4 Hz; ^{13}C carrier set to 118 ppm ($^{13}C^{\varepsilon}$), switched to 157.7 ppm ($^{13}C^{\zeta}$) immediately before and after the t_1 evolution period (50 complex t_1 increments), and then switched to 126 ppm (midway between $^{13}C^{\varepsilon}$ and $^{13}C^{\delta}$) for the remaining ^{13}C pulses. The ratio of detected $^{1}H^{\varepsilon}$ and $^{1}H^{\delta}$ intensities depends on τ_d. The duration and strength of the g_{10} gradient are 500 μs, 4 G/cm.

Quadrature detection in t_1 is obtained by States-TPPI incrementation of ϕ_3

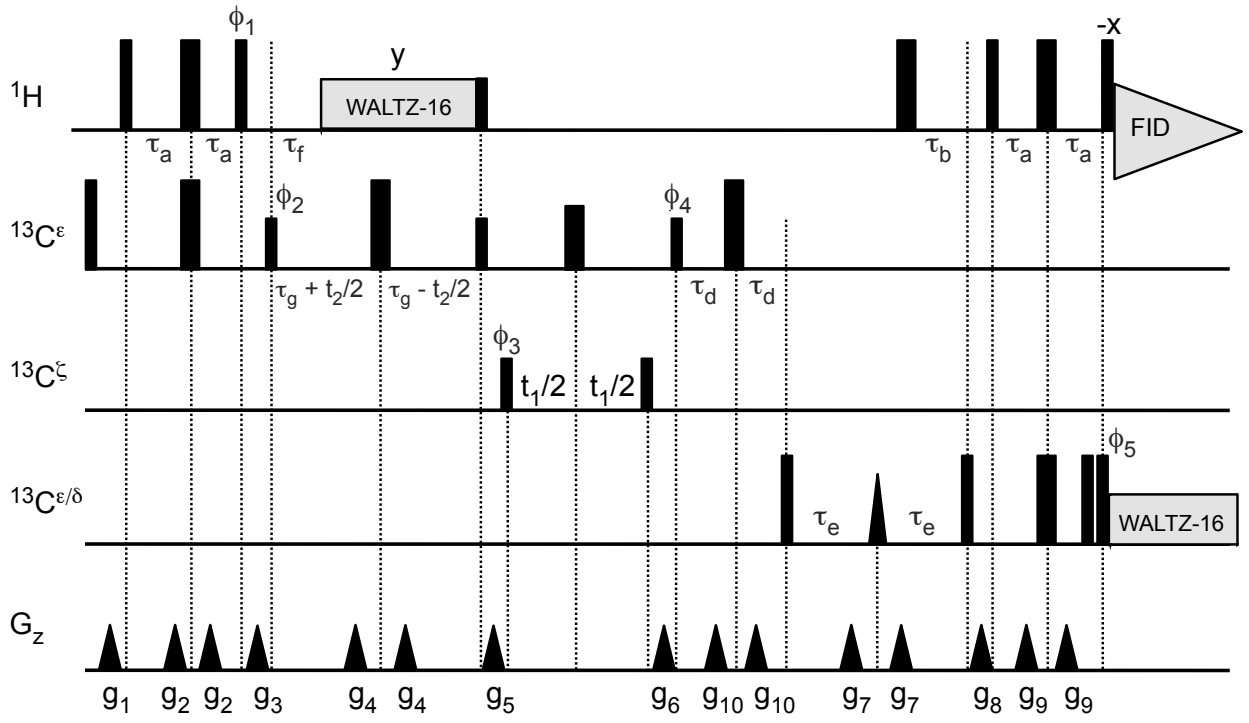

Fig. S8. The pulse sequence for a three-dimensional $^{13}C^{\zeta}{}^{13}C^{\varepsilon}(^{13}C^{\delta})^{1}H^{\varepsilon/\delta}$ experiment to correlate tyrosine $^{1}H^{\varepsilon/\delta}$, $^{13}C^{\varepsilon}$ and $^{13}C^{\zeta}$ signals (see Figure 6B). The magnetization transfer pathway is:

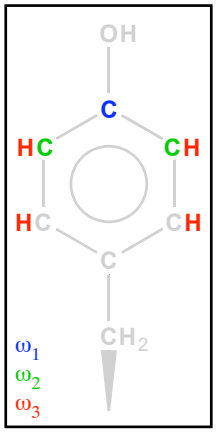

$$^{1}H^{\varepsilon}(t_3)$$
$$\uparrow$$
$$^{1}H^{\varepsilon} \rightarrow {}^{13}C^{\varepsilon}(t_2) \rightarrow {}^{13}C^{\zeta}(t_1) \rightarrow {}^{13}C^{\varepsilon} \rightarrow {}^{13}C^{\delta} \rightarrow {}^{1}H^{\delta}(t_3)$$

All parameters are the same as for the two-dimensional $^{13}C^{\zeta}(^{13}C^{\varepsilon/\delta})^{1}H^{\varepsilon/\delta}$ (Figure S7) with the following exceptions: additional delays $\tau_f = 2*\tau_b$ and τ_g = 19 ms; $^{13}C^{\varepsilon}$ spectral width of 905 Hz (25 complex t_1 increments, and 17 complex t_2 increments) using a 600 MHz spectrometer.

Quadrature detection in t_1 and t_2 is obtained by States-TPPI incrementation of ϕ_3 and ϕ_2, respectively.

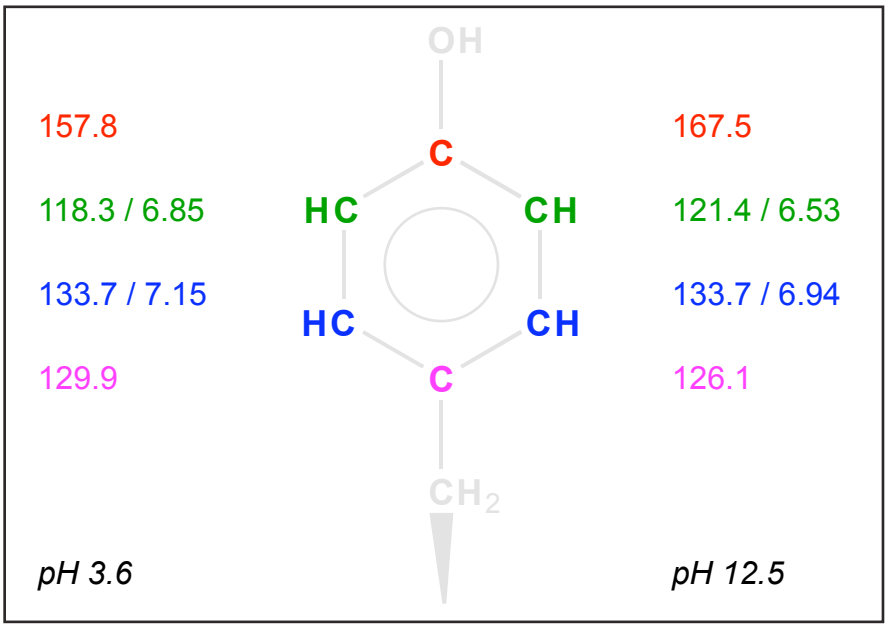

Fig. S9. The ^{13}C and ^{1}H chemical shifts (ppm) of free tyrosine at pH 3.6 and 12.5, measured from ^{13}C-HMBC spectra (10 mM sodium phosphate, 5% D_2O, 25 ^{o}C). These values agree with those reported for glycyl-L-tyrosine amide and glycyl-L-tyrosineglycine (Norton and Bradbury 1974), as well as tyrosine residues in a linear tetrapeptide Gly-Gly-Tyr-Ala (Richarz and Wüthrich 1978; Bundi and Wüthrich 1979). However, one exception is that a larger pH-dependent $^{13}C^{\gamma}$ chemical shift change ($|\Delta\delta|$ = 6.2 ppm or 6.8 ppm) is observed in the latter species, respectively, compared to the free amino acid.

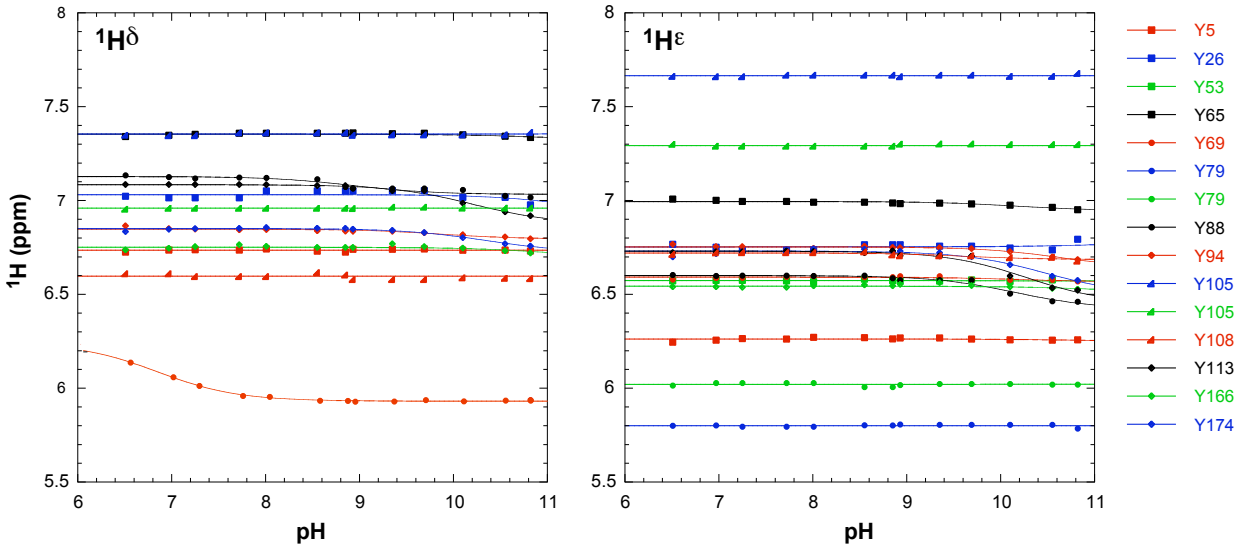

Fig. S10. The pH dependent $^{1}H^{\delta}$ (left) and $^{1}H^{\varepsilon}$ (right) chemical shifts of the BcX tyrosines (35 ^{o}C), measured from $^{1}H^{\varepsilon}/^{1}H^{\delta}$ ($^{13}C^{\varepsilon}$)$^{13}C^{\zeta}$ spectra. The lines represent the best-fits to a single titration event. In contrast to $^{13}C^{\zeta}$ (Figure 7), the $^{1}H^{\delta}$ and $^{1}H^{\varepsilon}$ nuclei show significantly more dispersion due to their structural environment than any changes due to the effects of pH, and thus their chemical shifts are not diagnostic of the tyrosine ionization states. Fitting the data for residues showing clear, albeit small, pH-dependent changes ($|\delta_b - \delta_a| > 0.1$ ppm) yielded the following apparent pK_a values:

Tyrosine	pK_a (from $^{1}H^{\delta}$)	$^{1}H^{\delta}$ Δδ (ppm)	pK_a (from $^{1}H^{\varepsilon}$)	$^{1}H^{\varepsilon}$ Δδ (ppm)
Y69	6.8 ± 0.1	-0.32		
Y88	8.9 ± 0.2	-0.10	10.2 ± 0.1	-0.18
Y94			10.7 ± 0.3	-0.12
Y113	10.2 ± 0.1	-0.21	10.3 ± 0.1	-0.28
Y174	10.4 ± 0.1	-0.13	10.5 ± 0.2	-0.23

Note that the fit pK_a values for Tyr113 and Tyr174 are similar for both the $^{1}H^{\delta}$ and $^{1}H^{\varepsilon}$, and also agree with those determined from their pH-dependent $^{13}C^{\zeta}$ shifts (Table 1). In contrast, whereas the $^{1}H^{\varepsilon}$ and $^{13}C^{\zeta}$ of Tyr88 yield comparable pK_a values, the $^{1}H^{\delta}$ appears to report the titration of other group(s) in BcX with a pK_a ~8.9; however, no obvious candidate can be identified from the crystal structure of the enzyme. The substantial change in the $^{1}H^{\delta}$ chemical shift of Tyr69 most likely reflects the ionization of the neighbouring catalytic general acid Glu172 (pK_a 6.7). (McIntosh et al. 1996; McIntosh et al. 2011)).

Supplemental References

Bundi A, Wüthrich K (1979) H-1-NMR parameters of the common amino-acid residues measured in aqueous-solutions of the linear tetrapeptides H-Gly-Gly-X-L-Ala-OH. Biopolymers 18:285-297

Farrow NA, Zhang O, Forman-Kay JD, Kay LE (1994) A heteronuclear correlation experiment for simultaneous determination of ^{15}N longitudinal decay and chemical exchange rates of systems in slow equilibrium. J Biomol NMR 4:727-734

Löhr F, Hansel R, Rogov VV, Dötsch V (2007) Improved pulse sequences for sequence specific assignment of aromatic proton resonances in proteins. J Biomol NMR 37:205-224

Löhr F, Rogov VV, Shi M, Bernhard F, Dötsch V (2005) Triple-resonance methods for complete resonance assignment of aromatic protons and directly bound heteronuclei in histidine and tryptophan residues. J Biomol NMR 32:309-328

McIntosh LP, Hand G, Johnson PE, Joshi MD, Korner M, Plesniak LA, Ziser L, Wakarchuk WW, Withers SG (1996) The pKa of the general acid/base carboxyl group of a glycosidase cycles during catalysis: a ^{13}C-NMR study of *Bacillus circulans* xylanase. Biochemistry 35:9958-9966

McIntosh LP, Naito D, Baturin SJ, Okon M, Joshi MD, Nielsen JE (2011) Dissecting electrostatic interactions in *Bacillus circulans* xylanase through NMR-monitored pH titrations. J Biomol NMR, in press

Norton RS, Bradbury JH (1974) C-13 nuclear magnetic-resonance study of tyrosine titrations. J Chem Soc Chem Comm:870-871

Richarz R, Wüthrich K (1978) Carbon-13 NMR chemical shifts of the common amino acid residues measured in aqueous solutions of linear tetrapeptides H-Gly-Gly-X-L-Ala-OH. Biopolymers 17:2133-2141